



Analyte kinetics in a nanocluster-based chemiresistor: A case study

M.G. Ancona*, A.W. Snow, F.K. Perkins, B. Pate, D. Park

Naval Research Laboratory, Washington, DC 20375, United States

ARTICLE INFO

Article history:

Received 22 August 2012

Received in revised form 8 November 2012

Accepted 26 November 2012

Available online 7 December 2012

Keywords:

Chemiresistor
Chemical kinetics
Gold nanoclusters
Amines
Diffusion

ABSTRACT

Nanoparticulate metal–insulator–metal ensemble chemiresistors in which the Au nanoclusters are functionalized with mercaptohexanoic acid are investigated as sensors of amines, and especially of triethylamine to which they are found to be extraordinarily sensitive with a minimum detectable level of less than 500 ppt. The dependences of the response on dose, time, and temperature are studied in detail. Modeling indicates that the entire data set is well explained by the interaction of partitioning and diffusion processes, both of which are temperature dependent.

Published by Elsevier B.V.

1. Introduction

Films of gold nanoclusters form the basis of an important class of chemiresistors known as MIME (for metal–insulator–metal ensemble) sensors [1–5]. The foundational element of these sensors is the gold nanocluster that, as depicted in Fig. 1 (upper left), consists of a gold core, typically a few nanometers in diameter, encapsulated by a monolayer of stabilizing ligands that are almost always attached to the gold surface via terminal thiol functional groups. When deposited on an insulating surface, a film of such nanoclusters can be electrically conducting as a result of electrons tunneling between the gold cores of neighboring clusters. Chemical-to-electrical transduction occurs when analyte enters the spaces between the cores, modulates the tunneling probability, and thereby affects the measured current. Although this general appreciation of MIME chemiresistance is solid, many details remain obscure including both the specific mechanisms of operation and how to improve that operation. As work toward further understanding, this paper presents a detailed case study of a particular MIME sensor that operates in an extraordinarily effective manner against its targeted analytes.

Among chemiresistive sensors, the MIME approach offers a unique combination of advantages. Foremost is its potential for high sensitivity due both to its high-gain transduction mechanism of tunneling modulation and to its nanocluster film implementation that accumulates signal by amassing huge numbers of tunnel junctions into the current path. A second critical advantage of the

MIME technology comes from the fact that the analyte interaction is strongly affected by the choice of the ligand forming the nanocluster coating. This carries considerable potential for enhancing the specificity of the response to particular analytes, and it also makes it possible to form arrays of MIME sensors with different functionalizations so as to enhance selectivity [6]. Other attributes of MIME sensors are the porosity of the nanocluster film and the monolayer nature of the cluster coatings, with both features facilitating the ingress/egress of analyte into the film and to the transductively active sites. A final advantage of the MIME design is that it is easily fabricated using simple micron-scale lithography on “any” insulating substrate followed by aerosol deposition of the clusters via air-brush or inkjet methods [7].

As reviewed in [4,5], there has been a considerable amount of work on MIME sensors with many different variants having been investigated. The most consequential feature of these sensors is the cluster coating which serves three major roles: (i) in synthesis/fabrication to stabilize the clusters against agglomeration during storage and aerosol deposition; (ii) in conduction/transduction to provide the insulating tunnel barriers whose modulation by the analyte constitutes the mechanism of operation; and (iii) in selectivity to build in affinity for certain analytes and/or aversion to interferents. A wide variety of ligands have been used as the coatings including alkanes [1–3], oxyethylenes [8], aromatics [2,9], rigid core interconnects [10], and perfluoroalkanes [11], and these ligands often incorporate functional groups such as thiols, halogens, ethers, alcohols, fluoroalcohols, phenols, nitriles, and amines [2,9].

The particular nanocluster employed in the MIME sensors studied in this paper has a gold core approximately 2 nm in diameter, a ligand shell of 1,6-mercaptohexanoic acid (MHA) (see Fig. 1), and

* Corresponding author.

E-mail address: ancona@estd.nrl.navy.mil (M.G. Ancona).

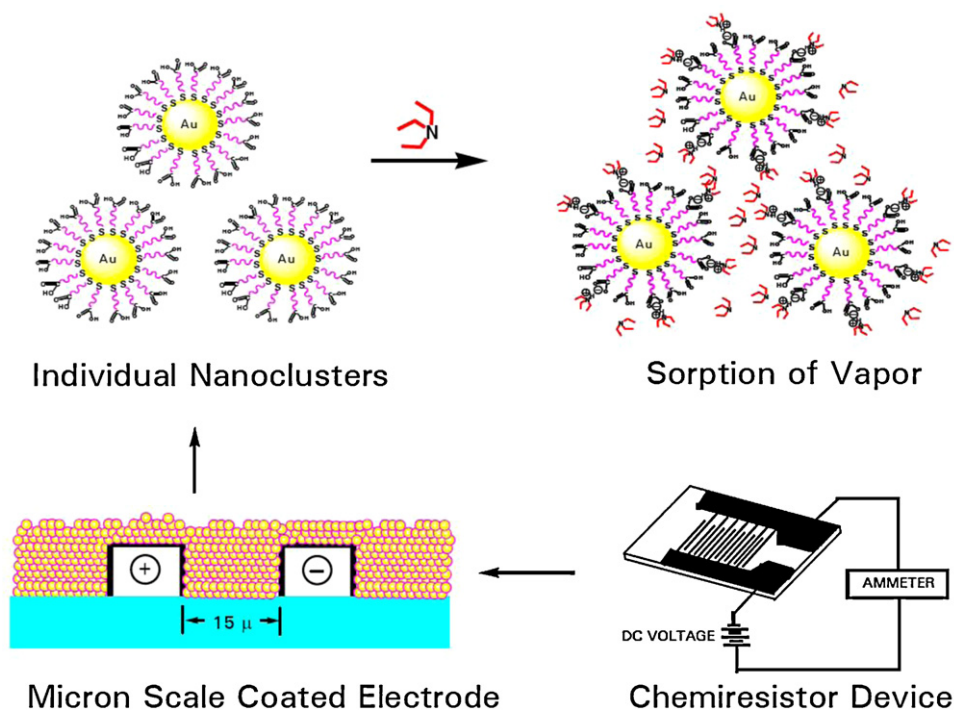


Fig. 1. Depictions of the COOH-functionalized nanoclusters and their integration into a MIM sensor.

is referred to by the shorthand Au:C₅COOH. MHA's thiol endgroup bonds the ligand to the gold core, and the carboxylate group at the distal end extends away from the core surface. A class of analytes that interacts strongly with the carboxylic acid receptor is the amines, and as a model system for this paper we focus primarily on triethylamine (TEA) due to its convenient vapor pressure, its simplicity and symmetry of molecular structure, and its unambiguous spectroscopic identity as a tertiary amine in an ammonium carboxylate complex. We find that a MIM sensor formed of MHA-coated clusters is extremely sensitive to TEA, responding to levels below one part-per-billion (ppb). In addition, this sensor exhibits a very wide dynamic range. Part of the value of trying to understand this sensor-analyte system is that it would obviously be highly desirable if one could learn how to incorporate similar performance into MIM sensors appropriate for other specific analytes.

The paper is organized as follows. In Section 2 we introduce and discuss the carboxylate-amine chemistry that forms the basis of the sensor under study. Section 3 details the experimental methods, and then the experimental sensor results are presented in Section 4. Modeling, analysis and discussion of the data follow in Section 5, and the paper closes with some concluding remarks.

2. Chemistry of the carboxylate-amine interaction

The specific interaction between TEA vapor and the carboxylic acid group of the MHA ligand is not well understood. That their combination should form a 1:1 ammonium carboxylate complex as depicted in Fig. 2a seems chemically intuitive [12], however, to our knowledge this complex has never been isolated. In an attempt to reach a more definitive understanding we conducted a series of reactions of carboxylic acids with tertiary amines (see Fig. 2b) aimed at realizing solid crystalline salts of well-defined stoichiometry that could then be analyzed. The first such experiment involved a 1:1 mixture of acetic acid and TEA, and unexpectedly it yielded a clear two-phase liquid mixture. This combination had been studied many years ago, both in solution [13,14] and as a neat mixture [15–17], and the latter work argued that the mixture was an

equilibrium between 1:1 and 1:3 amine:carboxylate complexes. But again a crystalline product did not form, so we then looked to favor such formation by substituting reactants with more rigid structures and higher melting points (see Fig. 2b). One attempt involved using benzoic acid (MP 122 °C) in place of acetic acid (MP 16 °C), but again this did not crystallize, even with prolonged cooling at –20 °C, and instead gave a single-phase viscous liquid. Likewise, substituting quinuclidine (MP 158 °C) for TEA (MP –115 °C) and reacting with benzoic acid produced a viscous liquid that did not crystallize after prolonged cooling at room temperature or –20 °C. In all cases these results were not due to an ammonium carboxylate complex failing to form since clear evidence for such a complex was seen in both the IR spectra (e.g., a reduction in intensity or disappearance of the C=O stretching band of the carboxylic acid at 1700 cm⁻¹, the appearance of bands corresponding to the carboxylate carbon-oxygen stretching at 1560 cm⁻¹ and the distinctive N–H stretching bands of the R₃NH⁺ ion at 2600 and 2500 cm⁻¹) and the NMR spectra (e.g., expected shifts in the resonances of nuclei in close proximity to the ionic centers associated with the ammonium carboxylate complexes). In any event, the isolation of a crystalline complex with a well-defined stoichiometry was not achieved. Hence the best understanding of the chemistry involved in the formation of the ammonium carboxylate complex continues to be that cited earlier [16,17].

Given the foregoing, the representation of the ammonium carboxylate complex formation in Fig. 2 is clearly an oversimplification, but it is still useful for interpreting IR spectra and for discussing the observed selectivity and sensitivity enhancements of the MHA-MIM sensor. To mimic the interaction of the –(CH₂)₅COOH moiety with TEA vapor experimentally (see Fig. 2a), we initially utilized a thin film of Br(CH₂)₅COOH deposited on a NaCl infrared window and obtained IR spectra both before and following a 15 min exposure to TEA vapor, and then after a further 15 min of heating at 80 °C. The pre-treatment spectrum (see Fig. 3a) displays a strong band at 1710 cm⁻¹ that is characteristic of the C=O stretching of the carboxylic acid and a weaker band at 940 cm⁻¹ that indicates that a significant percentage of the

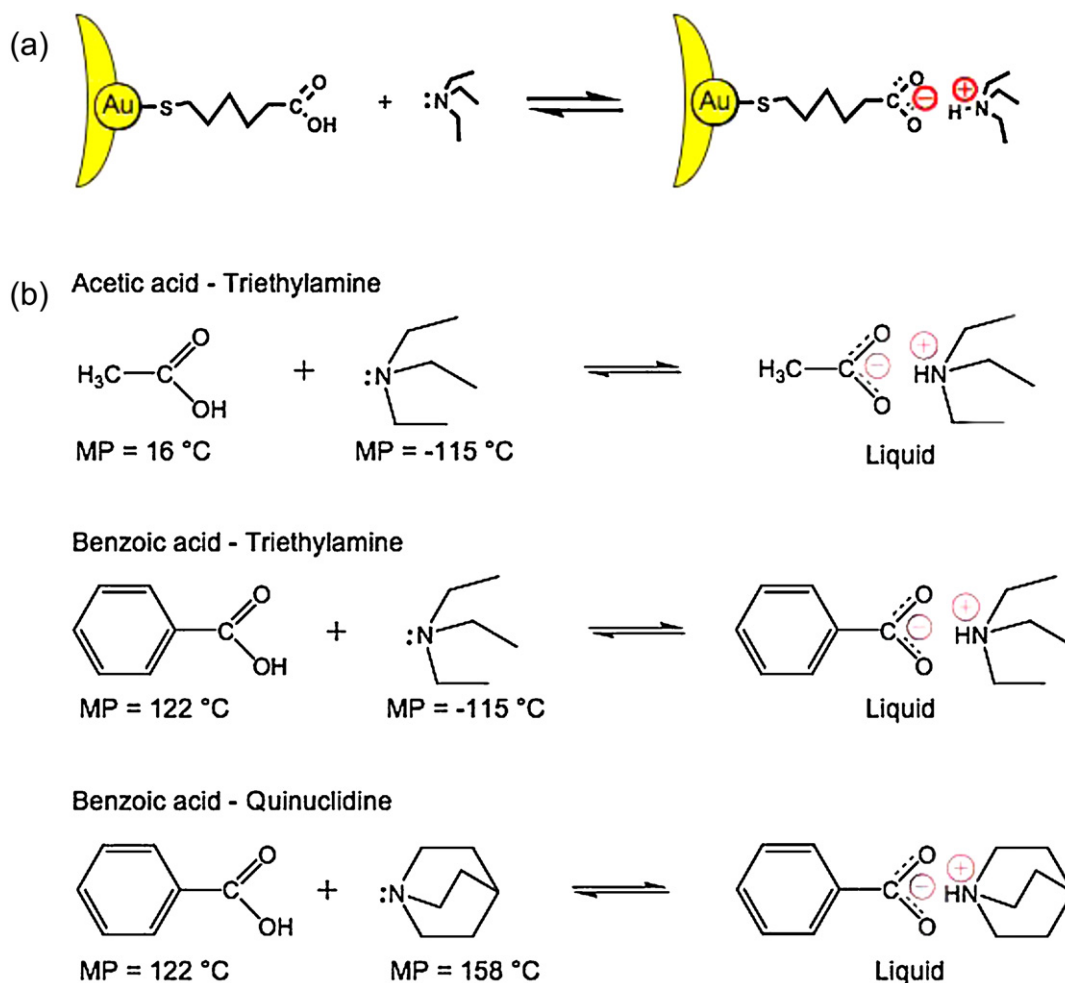


Fig. 2. COOH–amine complex formation (a) with TEA in the cluster film, and (b) in several model systems.

carboxylic acids are in the form of cyclic dimers [18,19]. Following exposure to TEA, the band at 1710 cm^{-1} is greatly reduced, the 940 cm^{-1} band disappears, and new bands appear at 1559 , 2497 and 2604 cm^{-1} . These changes are direct evidence of the formation of the ammonium carboxylate complex with the first new band being the C–O stretch [18,19] and the latter two bands being associated with the $\text{R}_3\text{N–H}^+$ stretching [20]. Ammonium carboxylate complexes are thermally labile and generally dissociate on mild heating; indeed, a brief warming of the film exposed to TEA restores the original spectrum (see bottom of Fig. 3a). An analogous set of experiments was conducted with a film of Au:C₅COOH clusters and the associated spectra (Fig. 3b) are similar to those on the Br(CH₂)₅COOH film (Fig. 2a) but with some differences. Specifically, prior to treatment the 1559 cm^{-1} band is present at low intensity, and the 940 cm^{-1} is absent. This would indicate that a small fraction of the carboxylic acid functional groups are ionized to the carboxylate form and are not in the cyclic dimer form. This latter result may be a consequence of the MHA ligand being surface bonded to the gold core of the cluster and not having sufficient flexibility to orient properly for dimer formation. Exposure of the Au:C₅COOH cluster film to TEA yields (see Fig. 3b) a large decrease in the 1710 cm^{-1} carboxylic acid band, the appearance of the 2497 and 2604 cm^{-1} $\text{R}_3\text{N–H}^+$ bands, and a marked increase in the 1559 cm^{-1} carboxylate band. A 15 min $80\text{ }^\circ\text{C}$ thermal treatment again dissociates the ammonium carboxylate complex and restores the original spectrum. With respect to the MHA–MIME sensor, it is the reversible formation of the ammonium carboxylate complex that provides

considerable selectivity to amines of sufficient basicity. And as we shall see, on a rapid purge/expose vapor testing cycle much of the reversibility occurs at room temperature and an elevated temperature accelerates the desorption.

3. Experimental methods

The synthesis/fabrication of the MIME sensors is much as described in previous work [1,2]. The Au:C₅COOH nanocluster was prepared by three successive ligand exchange reactions of HS(CH₂)₅COOH with a hexanethiol-stabilized 2 nm gold cluster [21]. This method was preferred over a direct Brust synthesis [22] because of difficulties the latter method has when the ligands have polar functional groups, both in controlling the Au core size and in separating the formed nanoclusters from the tetraoctylammonium bromide phase transfer agent. The substrates onto which these nanoclusters were deposited consisted of interdigitated gold electrodes defined on oxide-coated Si chips (see Fig. 1). The oxide was typically 100–200 nm thick and the interdigitated electrodes were about 500 nm thick, with finger/spacing dimensions of either $2\text{ }\mu\text{m}$ or $15\text{ }\mu\text{m}$, and with W/L of 32 000 in order to provide high sensitivity [23]. The electrodes were covered with a film of Au:C₅COOH nanoclusters deposited by an air-brush with a 10 mg/ml solution in methanol onto heated substrates (at $100\text{ }^\circ\text{C}$) [1]. Crude control of the film thickness comes from the number of $\sim 1\text{ s}$ passes by the air-brush. On a few samples a mechanical profilometer showed the

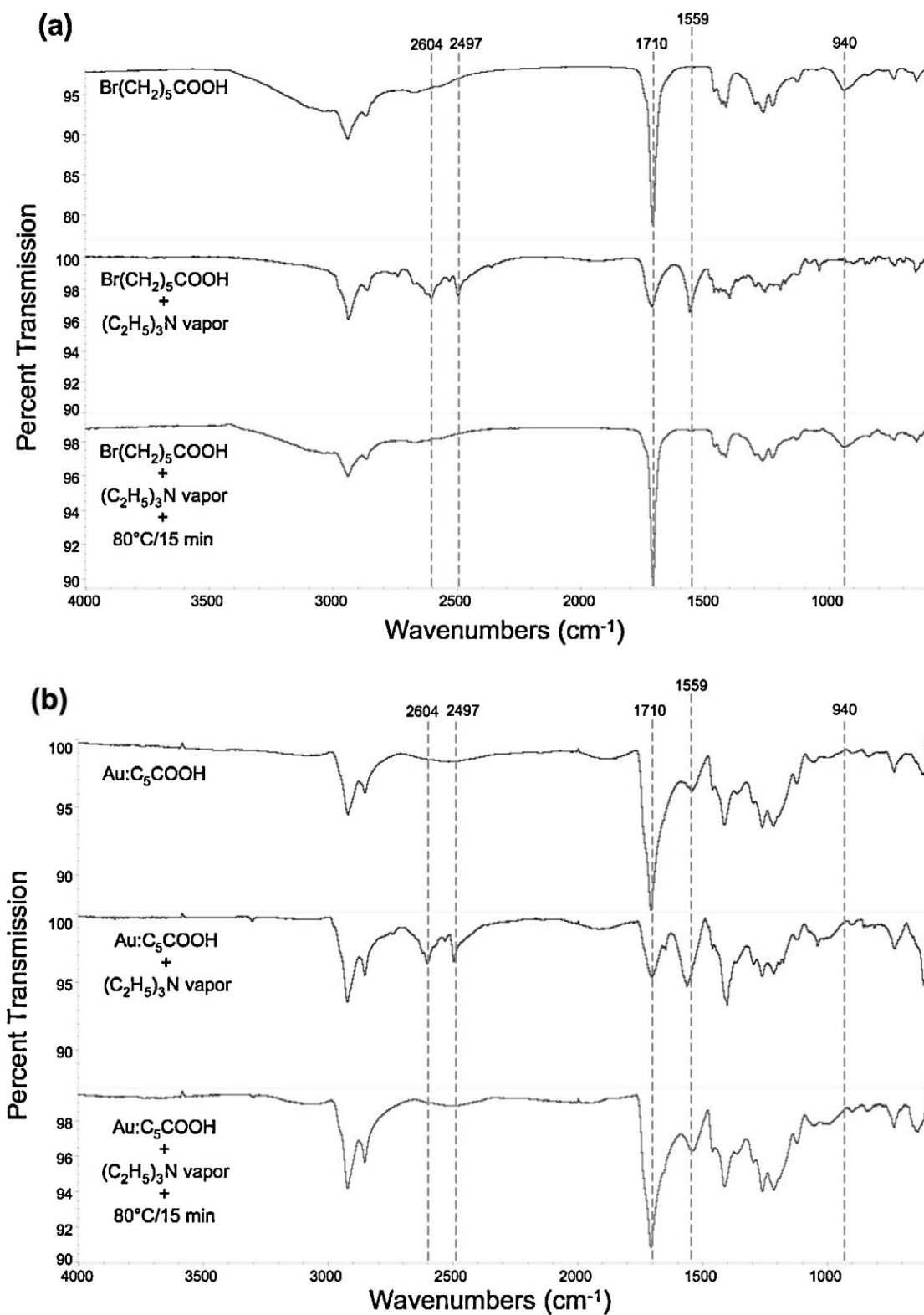


Fig. 3. IR absorption spectra (in percent transmission) of (a) a Br(CH₂)₅COOH film and (b) an Au:C₅COOH cluster film before, after exposure to TEA, and following heat treatment.

films ranged from about 0.1 to 1 μm in thickness and were quite rough due to the air-brush technique's deposition by droplets.

After an initial break-in period the sensors were found to be quite stable; in fact, a few test samples made 10 years ago and kept stored in a drybox remain functional. Also, the sensor characteristics appeared to be unaffected by brief heat treatments up to

about 80–90 °C, above which baseline shifts start to be seen. For this reason, all measurements in this paper were performed at sensor temperatures below 80 °C.

The TEA and other test analytes were obtained from commercial sources and distilled under nitrogen at 1 atm before use. Dosing was performed under computer control with the TEA delivered by

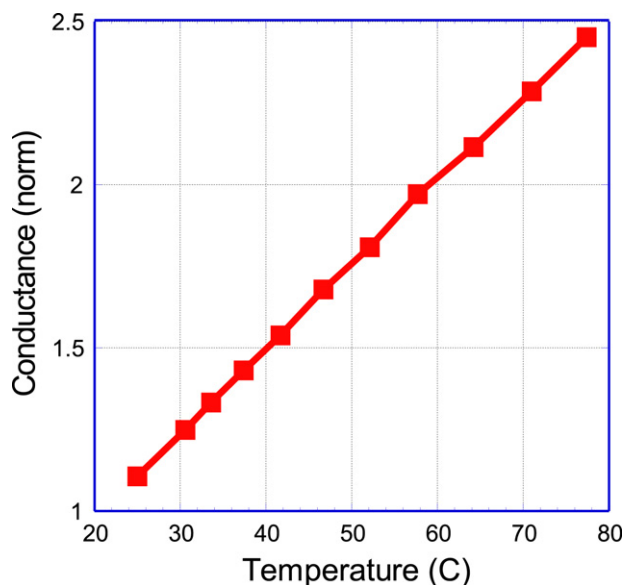


Fig. 4. The dependence of the conductance ($1/R_0$) of MHA-MIME sensors on temperature.

either a bubbler system at relatively high concentrations (>1 ppm) or a Kintek permeation tube system for very low concentrations (<100 ppb). The order-of-magnitude gap between these two ranges is obviously not desirable, but is characteristic of the delivery systems being used. In our work two bubbler-based vapor generation systems were used, one home-built and the other a Microsensor Systems, Inc. Model VG-400. In the former system, the vapor was delivered via a 3/16 in. dia. stainless steel pipe onto the sensor chip (from a distance of less than 1 cm) that sat on a heated chuck atop a manual probe station. The heated chuck provided temperature control with the temperatures monitored using thermocouples and/or an on-chip Au wire thermistor. The typical flow rate was 5 lpm with the analyte vapor being controllably switched in and out of the main flow by means of an electronically operated valve. For improved responsiveness the last few inches of the gas line are heated, thus inhibiting condensation of analyte on its walls. Au-coated tungsten probe tips were used to make electrical contact to the sensor, and ac conductivity was measured using a lock-in amplifier (Stanford Research Systems model SR830). The applied ac signal is a 0.1 V_{rms} sinusoid at a frequency of 2–3 kHz.

The numerical simulations were programmed and performed in MATLAB [24].

4. Sensor characteristics

When electrically contacted, the MHA-MIME sensor's Au:C₅COOH nanocluster film comprises a resistor, and the current through it is indeed found experimentally to be ohmic at low voltages, i.e., with a constant resistance R_0 . When the sensor is exposed to vapor this resistance changes by an amount ΔR , a quantity that represents the transductive response. For understanding the kinetics of this response, a crucial measurement in this paper is of how ΔR varies as a function of temperature. One complication that arises in interpreting such a measurement is that the MHA-MIME sensor's resistance is itself temperature dependent, in accord with the observations of [3] becoming increasingly conductive as the temperature rises as shown in Fig. 4. A standard expedient for handling this concern (as well as for nulling out other effects such sample-to-sample geometry variations) is simply to work with the normalized response $\Delta R/R_0$, and this approach is followed throughout this paper.

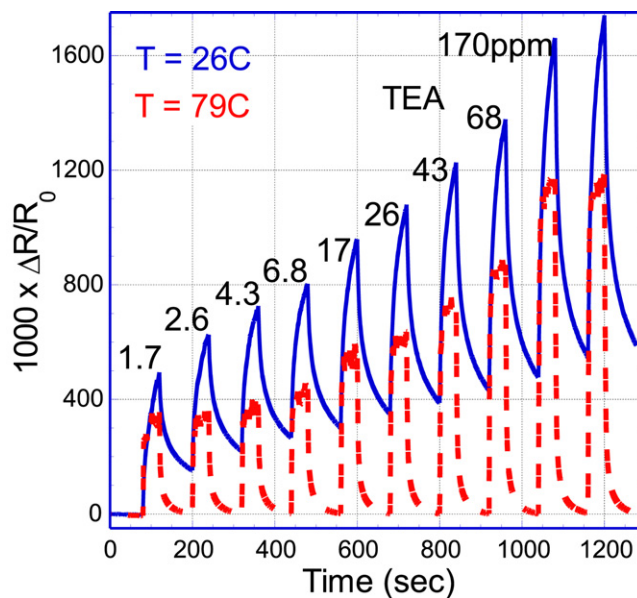


Fig. 5. MHA-MIME transient response curves to a sequence of doses at two different temperatures.

The basic response characteristic of a MHA-MIME sensor to TEA is shown in Fig. 5. The plot traces the transient variation in $\Delta R/R_0$ that occurs when the sensor is exposed to a sequence of vapor pulses (40 s on, 80 s off) as delivered by the bubbler system with the dose varying from 1.7 ppm to 170 ppm. Data are shown for two different sensor temperatures, 26 °C and 79 °C. At the higher temperature the response and recovery of the sensor to the various doses are seen to be quick and complete, whereas at lower temperatures a “non-recoverable” part is also observed. The latter fully recovers only after many hours and/or after heating. In all cases the magnitude of $\Delta R/R_0$ shows how strongly responsive the MHA-MIME sensor is to TEA.

To gauge exactly how sensitive the MHA-MIME sensor is to TEA, in Fig. 6 we plot the response isotherm obtained for varying doses after 40 s of exposure and with a sensor temperature of 26 °C. Data are shown both for higher exposures as delivered by the bubbler

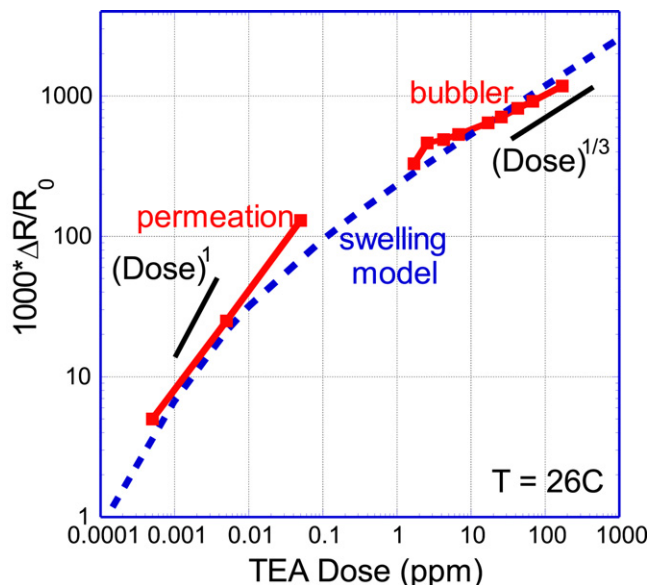


Fig. 6. Response isotherm for the MHA-MIME sensor showing both its high dynamic range and its sensitivity.

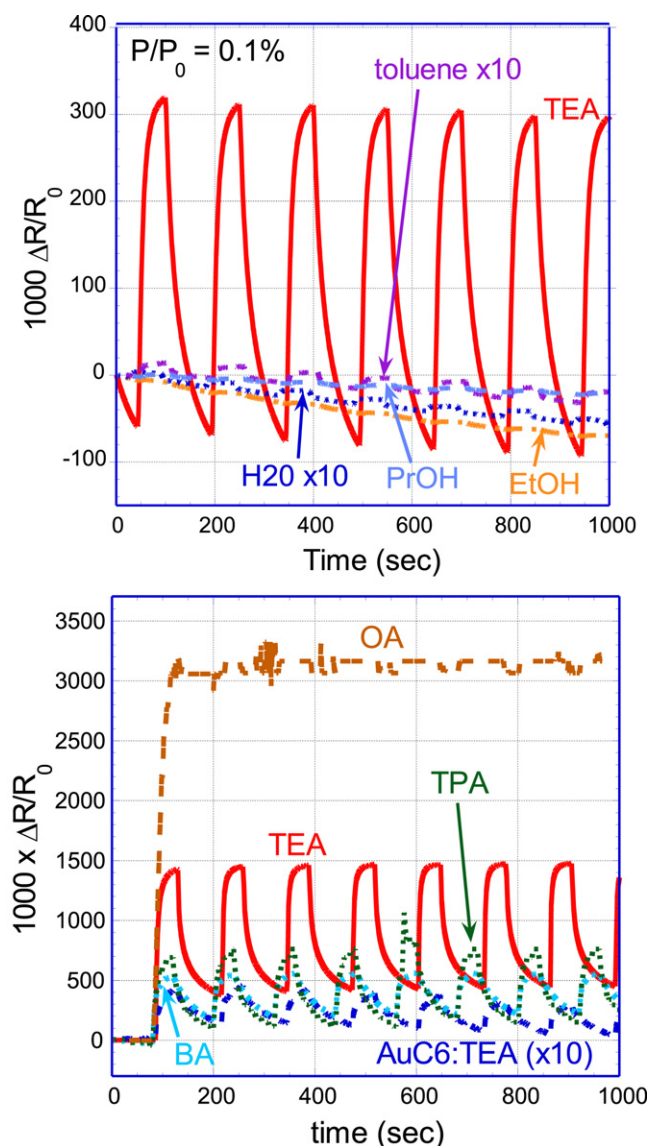


Fig. 7. (a.) MHA-MIME's selective TEA response to a sequence of fixed dose pulses compared with the much weaker responses observed to various non-amine containing vapors (water, toluene, 1-propanol, ethanol). (b.) An MHA-MIME sensor's strong response to TEA compared with its responses to other amines (BA: benzylamine, TPA: tripropylamine, OA: octylamine). Note that the OA response is almost completely irreversible at room temperature. Also shown is the weak response of a hexanethiol (Au:C6)-MIME sensor to TEA.

system and at lower doses as delivered from the permeation tube, with the gap in the ranges noted earlier being evident. From this plot the minimum detection limit can be estimated to be below 500ppt, an extremely low value for any chemiresistor technology. Moreover, as a sensor of TEA, Fig. 6 shows that the MHA-MIME device that has an extraordinarily high dynamic range, covering at least 7 orders of magnitude. Learning why this is an important reason for closer study of this system.

The strong response of the MHA-MIME sensor to TEA is attributed to the chemical complex formation discussed earlier that occurs between the carboxylic acid groups on the cluster surfaces and the amine-containing vapor. This is best seen by comparing the TEA response to that obtained for various other vapors with similar vapor pressures but with no amine functional group. To account for remaining differences in vapor pressure, we set the dose to be a fixed percentage of the equilibrium vapor pressure (in the bubbler headspace at 22 °C). As seen in Fig. 7a, for vapors that do not

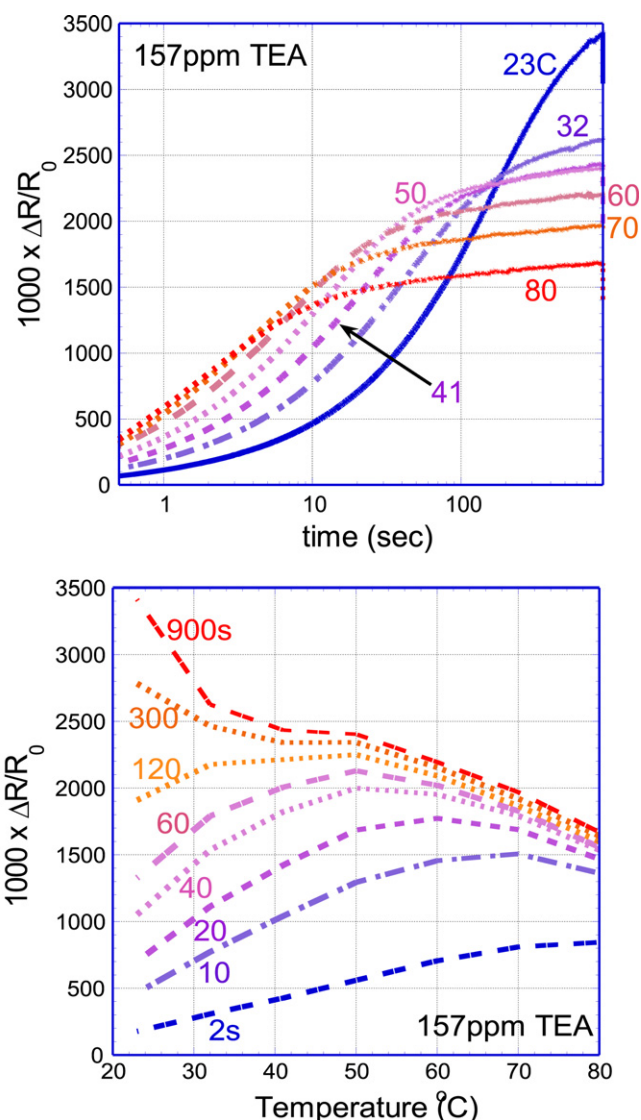


Fig. 8. (a.) Transient responses of an MHA-MIME sensor to a single 15 min dose of TEA (at 157 ppm) with temperature as a parameter. (b.) Cross-plot of the data in (a) with the time elapsed from the start of the exposure used as a parameter.

contain an amine the measured response to a vapor concentration of 0.1% is much weaker than it is for TEA. That such a weak response is seen for water vapor is especially important for sensor applications because of it being a ubiquitous interferent. When the exposure is instead made to vapors containing amine groups, Fig. 7b (here with a dose of 0.185%) shows responses that are comparable to that for TEA. For the vapors studied, Fig. 7a and b thus demonstrate that the MHA-MIME sensor is quite selective for amine-containing vapors. Lastly, to check on whether all MIME sensors show a preference for amines, we also examined the response of a sensor whose cluster film is formed of nanoclusters coated with hexanethiol ligands, i.e., with the same carbon chain length as MHA but without the carboxylic acid termination. The response to TEA is also plotted in Fig. 7b and it is found to be about a factor of 40 smaller than for the MHA-MIME sensor, again confirming the notion that it is the carboxylic acid–amine interaction that is key to the sensitivity/selectivity of the latter sensor for amines.

Next we examine in greater detail the dependence of the MHA-MIME sensor response to TEA vapor on sensor temperature. Fig. 8a shows the transient responses to a TEA dose of 157 ppm for duration of 900s and at various temperatures as indicated.

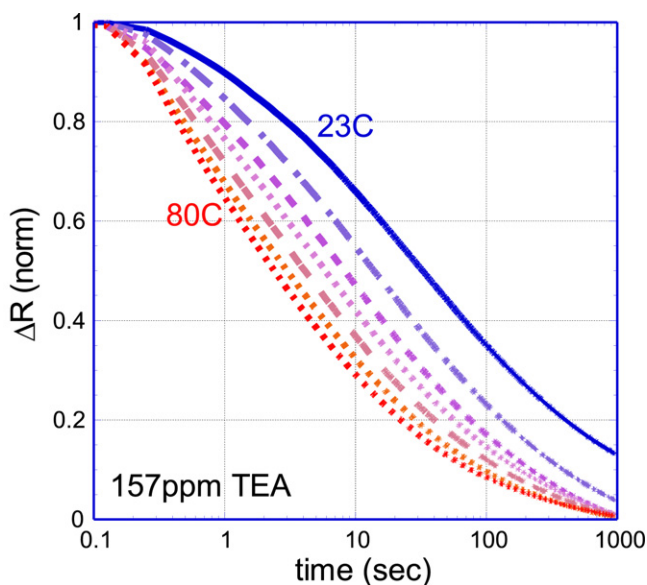


Fig. 9. Normalized recovery characteristics with temperature as a parameter following the termination of the exposure in Fig. 8.

Evidently as the temperature rises the response both accelerates and saturates at a lower level. As a consequence of this behavior, a cross-plot of these same data in Fig. 8b shows that, at relatively short times (<120 s), the response goes through a maximum at a particular temperature, a characteristic not ordinarily seen in MIME sensors.

The comparable plot to that of Fig. 8a for the recovery is shown in Fig. 9 with the ordinate normalized to the saturated value so as to remove the temperature dependence associated with the latter quantity. As with the response, we see that as the temperature rises the recovery speeds up.

Lastly, we examine the dependence of the response characteristics on the thickness of the cluster film. The data shown in Fig. 10 are analogous to the room temperature curve in Fig. 5 but for 10 repeated doses of 157 ppm (40 s on, 80 s off), and with two traces shown, one for a sensor (the same one as in Figs. 8 and 9)

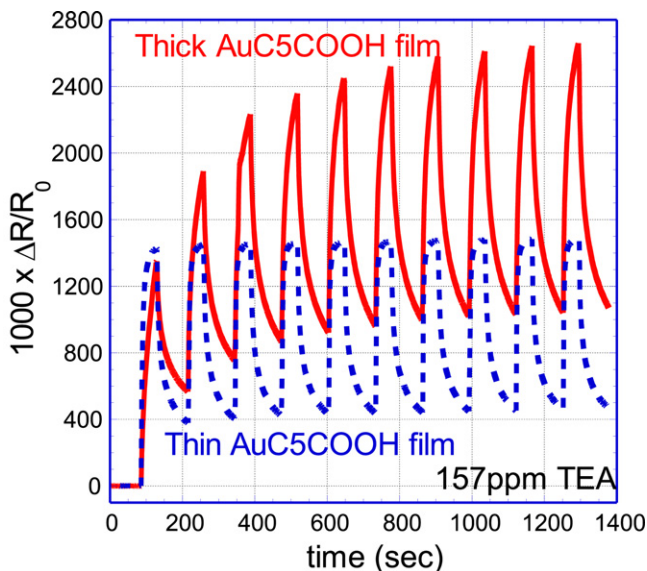


Fig. 10. Comparison of the dose response curves of MHA-MIME sensors to TEA for two different thicknesses of the nanocluster film at room temperature. The fixed dose is 157 ppm.

whose cluster film is roughly 0.5 μm thick and the other with a thinner film. As one might expect, the speed of the response is boosted when the film thickness is reduced. Interestingly, the “non-recoverable” part also quickens, so that in the thin-film case shown in Fig. 10 it is experienced almost entirely upon the initial exposure.

5. Theory of MIME sensor response

The basic picture of MHA-MIME sensor kinetics developed in this section is a straightforward one in which TEA analyte present as vapor in the ambient atmosphere enters the film, diffuses throughout its thickness, and as it does so, acts to modulate the film’s electrical conductivity. In order to model the observed sensor response and its dependence on time, dose, and temperature, it is therefore essential that we provide mathematical representations of the analyte’s entry into the film, its diffusion within the film, and the transduction process. For this purpose we designate the known TEA concentration outside the film (i.e., the dose) as c_0 , and the concentration inside the film as $c(x, t)$ with its uniform equilibrium value being c_{eq} .

5.1. Analyte entry

We assume that the entry of the analyte into the immediate top surface of the film occurs rapidly enough that it may be regarded as a quasi-equilibrium partitioning process whose magnitude is set by the common ambient/film temperature.¹ This allows us to use the concept of the equilibrium partition coefficient

$$K_p \equiv \frac{c_{eq}}{c_0} \cong \frac{c(0, t)}{c_0} = A_p 10^{-T/T_p} \quad (1)$$

to estimate the analyte concentration at the top surface of the film $c(0, t)$. The rightmost equality represents a commonly assumed form for the partition coefficient’s temperature dependence that, for example, provides an excellent description of the partitioning of dimethylmethylphosphonate (DMMP) into fluoropolyol [25] with T_p being a characteristic partitioning temperature and A_p being the pre-factor.

Diffusion. A simple model for the diffusion of TEA from the film’s top surface into its interior is provided by the one-dimensional diffusion equation:

$$\frac{\partial c}{\partial t} = D \frac{\partial^2 c}{\partial x^2} \quad (2)$$

where D is the diffusion constant. A significant assumption made in using this equation (and others below) is that the situation can indeed be regarded as one-dimensional, since as already noted the sprayed-on cluster film is quite rough.

Because of the strong interaction between the TEA molecules and the COOH groups in the cluster film as described earlier, it is natural to consider the diffusive transport as occurring via a “hopping” process in which individual TEA molecules proceed from one “binding” site (presumably consisting of one or more COOH groups) to another through the cluster film [26]. Eq. (2) can then be viewed as the Fokker–Planck equation that governs the continuum limit of this random walk. And if we assume an energy barrier E_a for hopping between TEA binding sites, then the diffusion will be temperature-activated with:

$$D(T) = D_0 \exp\left(-\frac{E_a}{kT}\right) \quad (3)$$

¹ This assumption will be violated if the analyte concentration is low enough that the arrival of molecules to the surface is insufficient to maintain the equilibrium.

5.2. Transduction

Little is known for certain about the transduction mechanism(s) of MIME sensors. Most commonly it is asserted that the primary mechanism is one in which a swelling of the cluster film occurs as the analyte vapor partitions into it, and this in turn modulates the MIME resistance by increasing the inter-core tunneling distances. Given the polar character of the COOH–amine complex, another plausible transduction mechanism is one based on a dipole modulation of the barrier height. However, it seems likely that this would manifest as a net barrier lowering and an increased current, whereas experiments involving the Au:C5COOH cluster always exhibit a decrease [27], and we therefore focus here on the swelling mechanism.

Turning the swelling concept into a detailed quantitative model is difficult because the swelling, like the film itself, is surely highly inhomogeneous. Moreover, the only swelling that will be important is that that occurs in the highly localized regions between closely spaced nanoclusters that are carrying appreciable current. To develop a crude model, we argue that since the inner portion of each cluster's shell will be well packed and relatively incompressible, the swelling-associated transduction must arise mainly from the “looser” outer regions where the cluster shells adjoin. Taking the average thickness of these latter regions to be d_0 and assuming that any swelling that occurs is isotropic, then the TEA-induced swelling will lead to an increase in volume of

$$\Delta V = (d_0 + \Delta d)^3 - d_0^3 = r_s c$$

where Δd is the increase in the inter-core (tunneling) distance produced by the swelling, and the second equality represents the reasonable assumption that the degree of swelling will be proportional to the analyte concentration. The proportionality constant r_s is a gross measure of the effectiveness of the analyte in both entering the transduction site and in causing swelling; presumably the former action is aided by the favorable energetics of the COOH–amine complexation, thus enhancing sensitivity. Mathematically, the preceding equation is a cubic in Δd and one can readily show that its only physically admissible solution is:

$$\Delta d = \sqrt[3]{d_0^3 + r_s c} - d_0$$

If Δd is small then the local increase in resistivity $\Delta \rho_s$ will be proportional (with proportionality constant $\partial \rho_s / \partial d \equiv \alpha_s$), and the resulting change in the resistance of the MIME sensor at time t can be represented by a “series model” and computed from

$$\begin{aligned} \Delta R(t) &= \frac{W}{L} \int_0^h \Delta \rho_s [c(x, t)] dx \\ &= \frac{W d_0 \alpha_s}{L} \int_0^h \left[\sqrt[3]{1 + r_s c(x, t) / d_0} - 1 \right] dx \end{aligned}$$

where W , L and h are the width, length and average thickness of the film, respectively, and the second equality incorporates the expression from our crude swelling model. For the analysis of the next section, it is helpful to define a normalized concentration $\tilde{c} \equiv c / c_{eq}$ in terms of which the diffusion problem is independent of c_{eq} . We then re-cast the previous equation into a more convenient form:

$$\frac{\Delta R(t)}{R_0} = a_\infty \left[\frac{1}{h} \int_0^h \sqrt[3]{1 + \tilde{c}(x, t) \frac{c_0}{c_\infty} 10^{(T_0 - T)/T_p}} dx - 1 \right] \quad (4)$$

where T_0 is a known “calibration temperature”, and a_∞ and c_∞ are composites of the earlier constants that are treated as fitting parameters. In steady state (i.e., after a long vapor exposure) we have:

$$\frac{\Delta R_\infty}{R_0} = a_\infty \left[\sqrt[3]{1 + \frac{c_0}{c_\infty} 10^{(T_0 - T)/T_p}} - 1 \right] \quad (5)$$

Taken together, the foregoing equations describing partitioning, diffusion, and transduction can in principle be solved to obtain the time, dose, and temperature dependences of the MIME sensor response. Checking these predictions against experiment would then support or refute the underlying physical/chemical models of the analyte behavior. The equations cannot be solved analytically, and so we employ a simple numerical scheme.

6. Analysis of sensor response

6.1. Steady-state behavior

After a MHA-MIME sensor has been exposed to TEA vapor for a “long” time, its response reaches a steady-state value as seen on the right side of Fig. 8a or the top curve in Fig. 8b. In normalized form the steady-state value is $\Delta R_\infty / R_0$, and according to the crude swelling model introduced in Section 5, the dose and temperature dependences of this quantity should be given by (5). Considering first the vapor concentration dependence as plotted in Fig. 6, we take $T = T_0$ to be room temperature and fit the data with (5) with the result, also shown in Fig. 6, being the dashed line. (The fact that the data of Fig. 6 is not taken under steady-state conditions is not expected to affect the basic trends, and especially given the crudeness of the swelling model on which (5) is based). The reasonable concordance means that the data are consistent with our model for the swelling mechanism. In particular, as (5) predicts, the dependence at low doses is roughly linear, whereas at high doses it rolls over into a power law with an exponent of 1/3. One important conclusion is that the significant signal compression and good performance at high TEA levels exhibited experimentally by the MHA-MIME sensor is simply a feature of the swelling process and arises because of its three-dimensional nature.

A second perspective on the TEA dose response and dynamic range of the MHA-MIME sensor can be obtained by comparing it with the response to other non-amine vapors. The plot in Fig. 11 shows that there is a general leftward shift in the TEA curve so that it rolls over into the 1/3 power “high” concentration regime at much lower doses than does the response to the other gases. Eq. (5) suggests that this will occur either because TEA partitions into the film more strongly (K_p is larger) and/or because the film is more efficient at transducing the TEA that enters it (r_s is larger or d_0 is smaller). Certainly both of these mechanisms would be aided by the amine-carboxylate affinity of the MHA-MIME sensor.

With respect to the temperature dependence of the steady-state response, a logarithmic plot of $\Delta R_\infty / R_0$ versus temperature in Fig. 12 shows this behavior to also be well described by (5). In particular, the best-fit straight line gives a partitioning temperature T_p of about 68 °C. This means that in its asymptotic behavior the MHA-MIME sensor follows the conventional picture of analyte partitioning between the vapor phase and the condensed phase of the cluster film, which causes the response to drop as the temperature increases. Clearly, at shorter times this is not the case (Fig. 8b) except at high temperature; in fact the behavior becomes peaked with a particular temperature at which the response is maximal. Our understanding of this behavior is that it is associated with the temperature-activated diffusion of TEA through the film as discussed in more detail next.

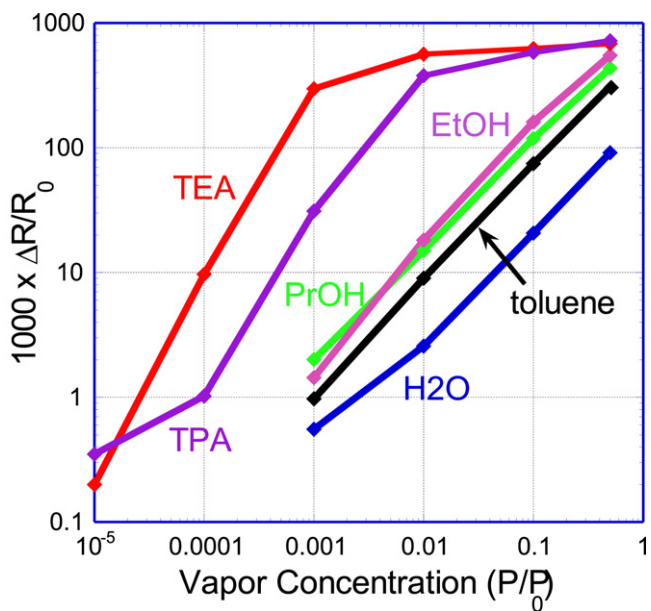


Fig. 11. Vapor response isotherms for an MHA-MIME sensor comparing the TEA response with that obtained for other vapors (water, toluene, 1-propanol, ethanol and tripropylamine).

6.2. Temporal response

We next consider the temporal response of the MHA-MIME sensor, e.g., as plotted in Fig. 8a. If the diffusion model is correct, this behavior should be described by (4). At a given temperature and with the various parameters estimated in the foregoing sections – h , a_∞ , c_∞ , and T_p – we are left with a single unknown parameter to be determined, namely, the diffusion constant D . In Fig. 13 we plot the data for $T=23^\circ\text{C}$ at a dose of 157 ppm of TEA together with simulated transients for various values of D . Evidently a value of D of about $7 \times 10^{-11} \text{ cm}^2/\text{s}$ gives a reasonable fit to the data. Performing similar fits to data at other temperatures (at the same dose), we find $D(T)$. An Arrhenius plot of these data in Fig. 14 shows it to be

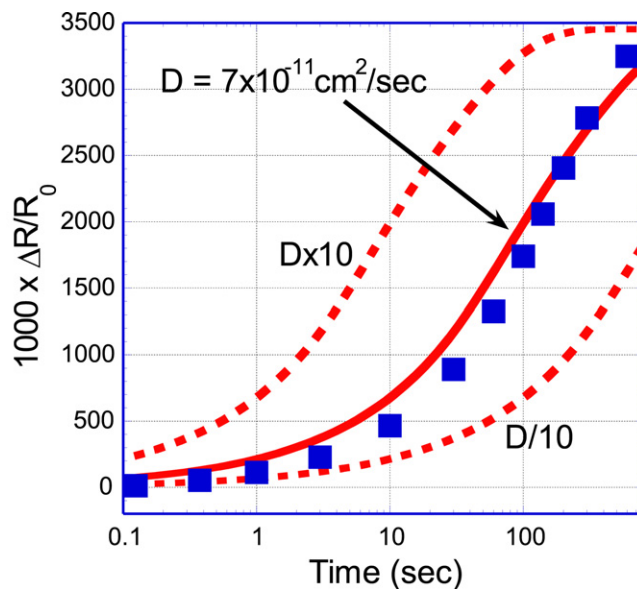


Fig. 13. The room temperature transient response curve from Fig. 8a along with simulated curves with varying values for the diffusion coefficient.

temperature-activated with an activation energy of approximately 0.69 eV.

6.3. Film thickness dependence

The dependence of the sensor's response on film thickness shown in Fig. 10 is readily analyzed using the equations of Section 5. Qualitatively, one expects that as the film thickness grows the behavior should become increasingly diffusion-dominated. And this is indeed what is seen experimentally. In Fig. 15 we plot the response time constants – defined as the time required for the response to rise to one-half its asymptotic value – as a function of h assuming that D takes the value noted earlier. The figure also provides estimates of the average film thicknesses of the devices characterized in Fig. 10.

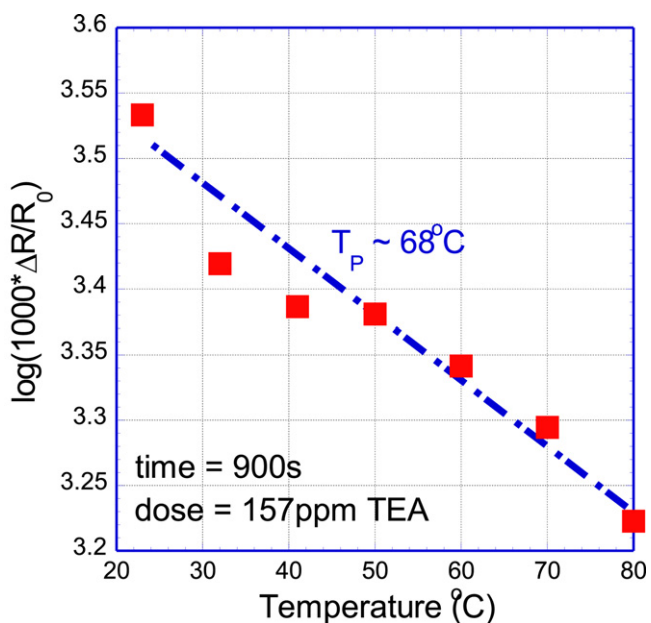


Fig. 12. Semi-log plot of the saturated response in Fig. 8 as a function of the temperature showing that it is well described by simple partitioning.

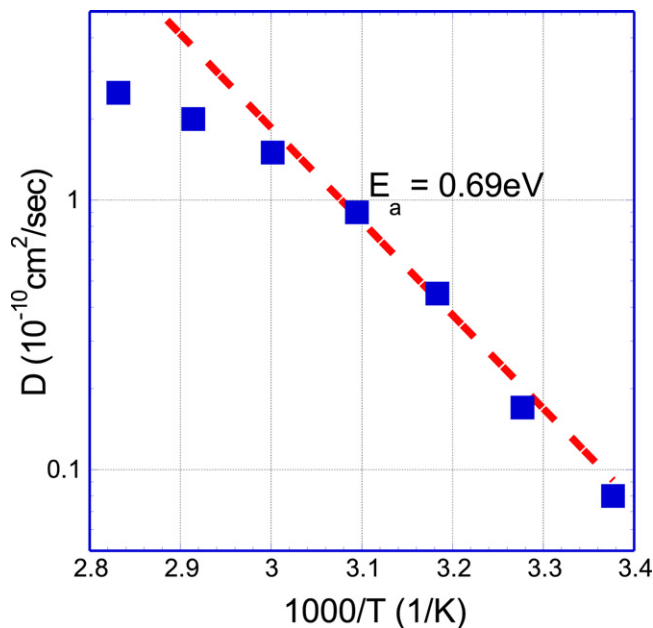


Fig. 14. The diffusion coefficients obtained by fitting the data of Fig. 8 as a function of $1000/T$, and showing that the behavior is well-represented by an activated diffusion.

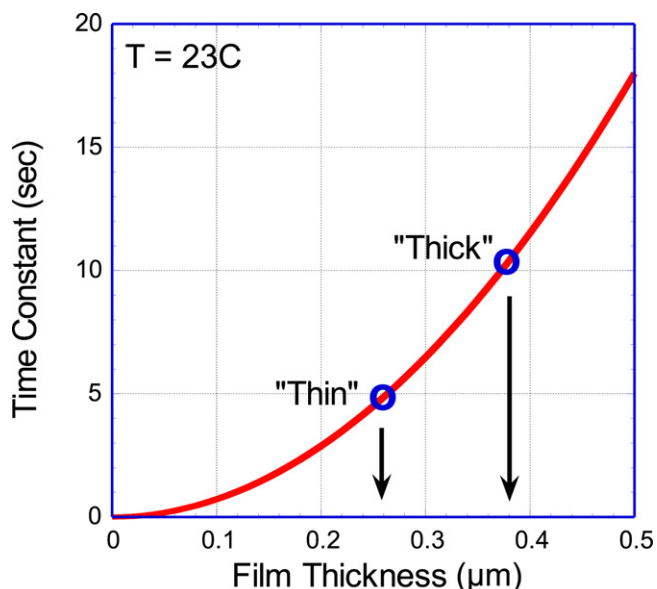


Fig. 15. Dependence of the simulated response time constant on the film thickness along with estimated experimental data for the cases in Fig. 10.

Fig. 15 shows that a thinner film gives a faster response and so would seem to be preferable. However, the performance is also affected by film thickness and so there is a trade-off. This comes about because, although our measure of sensor response $\Delta R/R_0$ is largely independent of geometry, this is merely the response "signal" and from a performance perspective the crucial parameter is the signal-to-noise ratio. Since the device operates at low frequency, the noise is generally $1/f$ noise that goes inversely with the square root of the sensor film's volume, and hence the minimum detectable concentration will be proportional to $1/\sqrt{WLh}$ [23]. We therefore expect a sensor of fixed lateral geometry but with a cluster film that is ten times thinner – and hence faster by a factor of 100 (see Fig. 15) – to have a minimum detectable concentration that is higher by a factor of three. And thus there is a trade-off between the speed of the MIME sensor response and its minimum detectable level. A second possible problem of a thinner film sensor is the increase in film resistance that can make the currents more difficult to measure (especially as we prefer to keep the applied voltages low).

7. Conclusion

MIME chemiresistors in which the Au nanoclusters are functionalized with 1,6-mercaptohexanoic acids are investigated as sensors of amines, and are found to be extraordinarily sensitive with a minimum detectable level of less than 500 ppt. The strong and selective response to amines is attributed to the complex formation that occurs between the carboxylic acid groups of the nanocluster ligands and the amine-containing vapor. The specific dependences of the response to triethylamine on dose, time, and temperature are studied in detail. Modeling indicates that all of these observations are well explained by the interaction of concurrent partitioning and diffusion processes, both of which are temperature dependent.

Although this paper is about the chemistry and physics of the MHA-MIME sensor, we close with the practical observation that the exceptional performance of this sensor as a detector of amine vapors could well have real-world applications. For example, trimethylamine vapor is a key analyte for assessing the state of freshness of fish and other proteinaceous foods, e.g., see [28].

Acknowledgement

The authors thank the Office of Naval Research for funding support.

References

- [1] H. Wohltjen, A.W. Snow, Colloidal metal–insulator–metal ensemble chemiresistor sensor, *Analytical Chemistry* 70 (1998) 2856.
- [2] A.W. Snow, H. Wohltjen, Materials, method and apparatus for detection and monitoring of chemical species, US Patents 6,221,673 (2001) and 7,347,974 (2008).
- [3] A.W. Snow, H. Wohltjen, Size-induced metal to semiconductor transition in a stabilized gold cluster ensemble, *Chemistry of Materials* 10 (1998) 947.
- [4] F.J. Ibanez, F.P. Zamborini, Chemiresistive sensing of volatile organic compounds with films of surfactant-stabilized gold and gold–silver alloy nanoparticles, *Small* 8 (2012) 174.
- [5] M.E. Franke, T.J. Koplin, U. Simon, Metal and metal oxide nanoparticles in chemiresistors: does the nanoscale matter? *Small* 2 (2006) 36.
- [6] G. Peng, U. Tisch, O. Adams, M. Hakim, N. Shehata, Y.Y. Broza, S. Billan, R. Abdah-Bortnyak, A. Kuten, H. Haick, Diagnosing lung cancer in exhaled breath using gold nanoparticles, *Nature Nanotechnology* 4 (2009) 669.
- [7] J. Im, S.K. Sengupta, J.E. Whitten, Photometer for monitoring the thickness of inkjet printed films for organic electronic and sensor applications, *Review of Scientific Instruments* 81 (2010) 034102.
- [8] E.E. Foos, A.W. Snow, M.E. Twigg, M.G. Ancona, Thiol-terminated di-, tri-, and tetraethylene oxide functionalized gold nanoparticles: a water-soluble, charge-neutral cluster, *Chemistry of Materials* 14 (2002) 2401.
- [9] A.W. Snow, H. Wohltjen, N.L. Jarvis, Metal–insulator–metal ensemble gold nanocluster vapor sensors, in: A.W. Miziolek, S.P. Karna, J.M. Mauro, R.A. Vaia (Eds.), *Defense Applications of Nanomaterials*, ACS Symposium Series 891, American Chemical Society, Washington, DC, 2005, pp. 31–45.
- [10] Y. Joseph, A. Peic, X. Chen, J. Michl, T. Vossmeier, A. Yasuda, Vapor Sensitivity of networked gold nanoparticle chemiresistors: importance of flexibility and resistivity of the interlinkage, *Journal of Physical Chemistry C* 111 (2007) 12855.
- [11] J. Im, A. Chandekar, J.E. Whitten, Anomalous vapor sensor response of a fluorinated alkylthiol-protected gold nanoparticle film, *Langmuir* 25 (2009) 4288.
- [12] H.C. Yang, D.L. Dermody, C. Xu, A.J. Ricco, R.M. Crooks, Molecular interactions between organized, surface-confined monolayers and vapor-phase probe molecules. 8. Reactions between acid-terminated self-assembled monolayers and vapor-phase bases, *Langmuir* 12 (1996) 726–735.
- [13] G.M. Barrow, E.A. Yerger, Acid–base reactions in non-dissociating solvents. acetic acid and triethylamine in carbon tetrachloride and chloroform, *Journal of the American Chemical Society* 76 (1954) 5211.
- [14] M. Wierzejewska-Hnat, Z. Mielke, H. Ratajczak, Infrared studies of complexes between carboxylic acids and tertiary amines in argon matrices, *Journal of the Chemical Society, Faraday Transactions II* 76 (1980) 834.
- [15] H.S. van Klooster, W.A. Douglas, The system acetic acid–triethylamine, *Journal of Physical Chemistry* 49 (1945) 67.
- [16] F. Kohler, E. Liebermann, G. Miksch, C. Kainz, On the thermodynamics of the acetic acid–triethylamine system, *Journal of Physical Chemistry* 76 (1972) 2764.
- [17] F. Kohler, H. Atrops, H. Kaijall, E. Liegermann, E. Wilhelm, F. Ratkovic, T. Salamon, Molecular interactions in mixtures of carboxylic acids with amines. 1. Melting curves and viscosities, *Journal of Physical Chemistry* 85 (1981) 2520.
- [18] N.B. Colthup, L.H. Daly, S.E. Wiberley, *Introduction to Infrared and Raman Spectroscopy*, 3rd ed., Academic Press, London, UK, 1990, pp. 313–315.
- [19] L.J. Bellamy, *The Infra-red Spectra of Complex Molecules*, 3rd ed., John Wiley & Sons, New York, USA, 1975, pp. 183–202.
- [20] M.A. James, T.S. Cameron, O. Knop, M. Neuman, M. Falk, Triethylammonium halides, Et_3NHX (X = Cl, Br, I): simple structure, complex spectrum, *Canadian Journal of Chemistry* 63 (1985) 1750.
- [21] A.W. Snow, M.G. Ancona, D. Park, Nanodimensionally driven analyte response reversal in gold nanocluster chemiresistor sensing, *Langmuir* (2012), <http://dx.doi.org/10.1021/la303319j>, Article ASAP.
- [22] M. Brust, M. Walker, D. Bethell, D.J. Schiffrin, R. Whyman, Synthesis of thiol-derivatized gold nanoparticles in a 2-phase liquid–liquid system, *Journal of the Chemical Society: Chemistry Communications* (1994) 801.
- [23] M.G. Ancona, A.W. Snow, E.E. Foos, W. Kruppa, R. Bass, Scaling properties of gold nanocluster chemiresistor sensors, *IEEE Sensors Journal* 6 (2006) 1403.
- [24] See <http://www.mathworks.com/>
- [25] J.W. Grate, A.W. Snow, D.W. Ballantine, H. Wohltjen, M.H. Abraham, R.A. McGill, P. Sasson, Determination of partition-coefficients from surface acoustic-wave vapor sensor responses and correlation with gas–liquid chromatographic partition-coefficients, *Analytical Chemistry* 60 (1988) 869.
- [26] W.H. Steinecker, M.P. Rowe, E.T. Zellers, Model of vapor-induced resistivity changes in gold–thiolate monolayer-protected nanoparticle sensor films, *Analytical Chemistry* 79 (2007) 4977–4986.
- [27] Interestingly, sensors made with larger COOH–clusters exhibited a complete reversal of this behavior as discussed in [21].
- [28] P.-M. Schweizer-Berberich, S. Vaihinger, W. Göpel, *Sensors and Actuators B* 18–19 (1994) 282–290.

Biographies

M.G. Ancona is a research physicist in the Electronics Science and Technology Division of the Naval Research Laboratory. His research interests include nanoelectronics, chemical sensors and computer modeling.

A.W. Snow graduated from Michigan State University with a B.S. in chemistry in 1971, followed by brief military service, then graduated from the City University of New York in 1977 with a Ph.D. in polymer chemistry. After a year at American Cyanamid Company, he came to the Naval Research Laboratory as a National Research Council Research Associate in 1978 and became an NRL staff member as a research chemist in 1979. His research interests are polymer synthesis, electroactive polymers, low-dielectric polymers, chemical microsensors, metal nanoclusters and nonlinear optical materials.

F.K. Perkins received an SB in Physics from MIT in 1982, and MS and PhD. in Materials Science from the University of Wisconsin-Madison in 1988 and 1992, respectively.

Since 1992 he has worked in the Electronics Science and Technology Division of the Naval Research Laboratory. His research interests have varied from the very large, extra-galactic supernova remnants, to the very small, atomic site-defects in carbon nanotubes (CNTs). His current research lies in the application and optimization of CNTs for chemical sensors and RF devices.

B. Pate is a research physicist in the Chemistry Division of the Naval Research Laboratory. His research interests include spectroscopic characterization and diamond growth.

D. Park received the B.S. and M.S. degrees in Electrical Engineering from the University of Maryland, College Park, MD in 1983 and 1986, respectively. In 1985, he joined the Naval Research Laboratory as an Electronics Engineer where he is engaged in the development of HEMT and NEMS/MEMS devices. His current research interests include advanced e-beam lithography techniques and nanoelectronic device design and fabrication.